NON-OXIDATIVE TORREFACTION OF BIOMASS TO ENHANCE ITS FUEL PROPERTIES

Ana Alvarez, Dositeo Nogueiro, Consuelo Pizarro*, María Matos, Julio L. Bueno

Department of Chemical and Environmental Engineering, Faculty of Chemistry, University of Oviedo, Julián Clavería 8,33006 Oviedo, Asturias, Spain

**corresponding author*

Email address: pizarroconsuelo@uniovi.es

ABSTRACT

Torrefaction upgrades the biomass as an energy source enhancing its poorest characteristics. Non-oxidative torrefaction of six biomass samples (pine, eucalyptus, chestnut, holm oak, olive tree pruning and vine shoot) was conducted in a tube furnace reactor within the range 200-300 ºC and proximate, ultimate and heating value analysis as well as wettability studies were carried out to characterize the torrefied samples and find the optimal temperature of the process. In addition, Pyrolysis-gas chromatography/mass spectrometry (Py-GC/MS) was performed and chemical-kinetics parameters of torrefaction were obtained at optimal temperature. At optimal torrefaction temperature, moisture was reduced up to 2.5 % and H/C and O/C atomic ratios up to 1.3 and 0.6, respectively. Contact angle measurements show an increase in hydrophobic behaviour. Lignin was affected by torrefaction since decomposition products from guaiacyl (G) and syringyl (S) units were released during Py-GCMS experiments. The global reaction order was 2.2 and kinetic constant values

were in the range $2.17 \cdot 10^{-5}$ to $4.83 \cdot 10^{-5}$ s^{-1}.

KEYWORDS: torrefaction, proximate analysis, ultimate analysis, Py-GC/MS, hydrophobicity, contact angle, torrefaction kinetics

1. INTRODUCTION

Biomass is one of the promising renewable energy sources which provides 10% of world primary energy supply [1] and contributes to match the European targets by 2020. It has a higher availability than other renewable energy sources such as wind and hydropower [2]. However, biomass is characterized by its hygroscopicity and compared to coal it has lower calorific value and lower energy density, which may cause problems in its transport, storage and combustion. Furthermore, its fibrous nature results in a difficult grinding, which requires higher energy input than coal.

In order to overcome these undesirable properties, biomass can be pretreated via torrefaction. Dry non-oxidative torrefaction is a mild pyrolysis process carried out at temperatures ranging of 200-300 ºC in an inert atmosphere [3]. Torrefied biomass possesses better properties as fuel than raw biomass. Improvements after torrefaction include lower moisture content, higher high heating value (HHV), and the torrefied biomass turns hydrophobic [4]. As a result, energy density of torrefied biomass is increased and its grindability improved [5]. In addition, its susceptibility to biological degradation is reduced due to the acquired hydrophobic nature of torrefied biomass. Hydrophobic behaviour of raw and torrefied biomass can be measured by wettability studies. Contact

49 angle is considered to correlate with the wettability of surfaces. The topic of
50 wetting plays an important role in many industrial processes, such as oil
51 recovery, lubrication, coating and painting [6–11]. Wettability studies usually
52 involve the measurement of contact angles as the primary data, which indicates
53 the degree of wetting when a solid and liquid interact. Small contact angles
54 (<90°) correspond to high wettability, while large contact angles (>90°)
55 correspond to low wettability [10]. Many of the differences in contact angle
56 values are reported to be largely attributed to surface roughness differences of
57 the different species and different wood surfaces [6,7]
58 Py-GC/MS is appropriate for studying biomass torrefaction components
59 evolving, though this technique is mainly used in pyrolysis studies rather than
60 torrefaction ones. As known, lignin of woody biomass is mainly composed of
61 guaiacyl (G) and syringyl (S) units and in a lesser extent p-hydroxyphenyl (H)
62 units. Py-GC/MS has been increasingly used to estimate the S/G ratio of lignin.
63 A few studies have been conducted focused on how the torrefaction affects the
64 structural components of biomass and its torrefaction kinetics [4,5,12]. The
65 results showed that hemicellulose is the most reactive component of biomass
66 even at low temperatures and the reaction order of xylan was found as third
67 order. With regard to the standard fuel analysis, mass and energy yields, there
68 has been a great deal of research [2,13–17]. Several papers study the kinetics
69 of torrefaction through single step [4] or two-step models [18–21]. A few studies
70 report on the improvement of their grindability properties [17,22,23]. Py-GC/MS
71 was used to study the evolved gases during the pyrolysis of several kinds of
72 biomass such as pine sawdust [24], silver birch sawdust [25] or poplar wood

sawdust [26]. There have not been found Py-GC/MS experiments at torrefaction temperature nor wettability studies of torrefied biomass. Most of the researches made in torrefaction is focused on torrefaction of pine, eucalyptus, chestnut [2,22,27–34] and olive tree [35]. However, there have been found no studies on holm oak or vine shoot, which are some of the main types of residual biomass in Spain and other Mediterranean countries.

The present study focuses on the non-oxidative torrefaction of these last 6 samples, i.e. pine, eucalyptus, chestnut, olive tree, holm oak and vine shoot. Mass and energy yields, proximate and ultimate analyses and high heating value were obtained, the hydrophobicity was assessed and an optimal torrefaction temperature was found based on these results. In addition, gases from torrefaction were analysed by Py-GC/MS at the optimal torrefaction temperature found. Furthermore, isothermal kinetics of torrefaction at the optimal temperature were calculated using a thermogravimetric analyser.

2. MATERIAL AND METHODS

2.1 Sample preparation

Six woody biomass samples were used in this study, which are pine, eucalyptus, chestnut, holm oak, olive tree pruning and vine shoot. These samples have been chosen to ensure that the main forestry and agroindustrial wastes in many European countries were studied. Biomass samples were grinded and sieved to a size between 710 - 1000 μm and the characterization of the raw biomass samples were conducted (Table 1).

Table 1. Characterization of raw biomass samples.

	Pine	Eucalyptus	Chestnut	Vine shoot	Holm oak	Olive tree pruning
Proximate analysis, %						
Moisture	7.63	9.45	7.85	7.63	9.31	9.07
Volatiles	87.87	84.20	82.17	74.13	78.27	81.95
Ash	0.25	1.54	0.13	12.10	3.31	2.82
Fixed Carbon	11.88	14.26	17.70	13.77	18.42	15.23
Ultimate analysis, %						
C	47.90	44.91	46.35	42.15	45.22	44.49
N	0.16	0.29	0.20	0.88	0.64	0.63
S	0.51	0.54	0.98	0.71	0.62	0.64
H	6.53	6.24	6.00	5.86	6.05	6.27
O	44.89	48.03	46.48	50.41	47.46	47.97
HHV, J/g	19402	17655	17687	16487	17537	18007

2.2 Torrefaction experiments

Pine, eucalyptus and chestnut were the samples selected for determination of optimal torrefaction temperature. Non-oxidative torrefaction experiments were carried out in a tube furnace reactor (Carbolite MTF 12/38/150) and inert atmosphere at five different temperatures (200, 225, 250, 275 and 300 °C, except for chestnut with only 225, 250 and 275 ºC experiments). The temperature of the reactor was raised to the selected temperature by a linear heating rate of 20 °C min^{-1}, and held for 20 min at that temperature meanwhile a constant N_2 flux of 1 l min^{-1} was used as the inert gas. Five to eight replicates were done. Once the optimal torrefaction temperature has been determined, the pretreatment was applied to the rest of the samples at this temperature and mass and energy yields were checked to be similar to those of pine, eucalyptus and chestnut.

2.3 Solid analysis

Proximate and ultimate analysis were performed on torrefied samples, as well as the heating value. Proximate analysis and heating value were carried out according to the ASTM Standards [36–39] in a muffle furnace (Carbolite CWF 1100) while ultimate analysis was conducted using an elemental analyser (Elementar Vario Macro CHNS).

Hydrophobic behaviour was studied through wettability tests carried out using eucalyptus samples due to the wider temperature range of torrefaction experiments available and the fact that this sample is representative of the rest of the samples studied in this paper, except pine. Initially 600 mg of torrefied eucalyptus at temperatures between 200 ºC and 300 ºC as well as raw eucalyptus were pressed into pellet with 13 mm in diameter using a hydraulic press (Specac) under the pressure of 5 metric tons. Contact angles (θ) on pellet surfaces were measured using a CAM 200 optical contact angle meter (KSV Instruments Ltd.). Sessile water droplets were placed on the wood pellet by a syringe and allowed to spread freely on the surface. Spreading images were captured by a high-resolution CCD camera at 40 ms intervals for 0.4 s. Contact angles were determined using the KSV CAM 200 software.

2.4 Gas analysis

Gases produced at optimal torrefaction temperature of the samples were characterized using pyrolysis gas chromatography/mass spectrometry (Py-GC/MS). For this assay, a micro-furnace type double-shot pyrolyzer model PY2020iD (Frontier Lab Ltd.) attached to a GC/MS system Agilent 6890 was

used. Samples (4 mg) were placed in small crucible capsules and introduced in a pre-heated furnace (240 °C) in the absence of oxygen. The sample was kept for 2 minutes at this temperature before the evolved gases where directly injected in the GC/MS for analysis.

The GC was used with a fused silica capillary column HP 5MS (30 m × 250 μm × 0.25 μm inner diameter), oven temperature was held at 50 °C for 1 min and then increased up to 100 °C at 30 °C min-1, from 100 to 300 °C at 10 °C min-1 and isothermal at 300 °C for 10 min in the scan modus. The carrier gas used was helium with a controlled flow of 1 ml min^{-1}. The detector consisted of an Agilent 5973 mass selective detector and mass spectra were acquired with a 70 eV ionizing energy within the scan interval 50-550 m/z.

Compound assignment was achieved via single ion monitoring for different homologous series, low resolution MS and comparison with published and stored (NIST and Wiley libraries) data. Semi-quantitative calculations were performed on the pyrograms, by integrating the chromatographic peaks corresponding to identified compounds and converting the obtained areas into relative percentages. The type of the biogenic compound were also indicated.

2.5. Kinetics of torrefaction

4 mg of the sample were subjected to thermal decomposition at optimal torrefaction temperature in a Perkin-Elmer STA 6000, using 200 ml min^{-1} of N_2 as carrier gas and the temperature program described by Chen and Kuo [4].

3. RESULTS AND DISCUSSION

3.1. Determination of optimal torrefaction temperature and torrefaction of

biomass

Firstly, the optimal temperature of torrefaction was determined. The mass and energy yields of the selected samples (pine, eucalyptus and chestnut) subjected to different torrefaction conditions were in the range between 54.3 - 91.8 % and 71.9 - 98.4 % respectively (Table 2). It is widely accepted that the optimal balance of mass and energy for biomass torrefaction is 80 % of mass yield and 90 % of energy yield in the torrefied biomass [28,40,41], thus the optimal torrefaction temperature have to meet this two requirements.

Table 2. Mass and energy yields and HHV values for optimal torrefaction temperature determination (dry basis).

Sample	Temperature, ºC	HHV, J/g	Mass yield, %	Energy yield, %
Pine	200	20359	91.8	96.4
	225	20580	90.6	96.1
	250	21130	85.6	93.2
	275	21268	79.3	86.9
	300	22973	65.9	78.1
Eucalyptus	200	19055	90.6	97.8
	225	19649	87.4	97.2
	250	20303	77.9	89.5
	275	21394	69.0	83.6
	300	23342	54.3	71.9
Chestnut	225	19905	87.4	98.4
	250	20872	75.7	89.4
	275	21445	68.6	83.2

Furthermore, linear relationship between mass yield and torrefaction temperature (Figure 1) and mass and energy yields (Figure 2) were found. These results suggest that woody biomass behaves similarly and therefore it is easier to find the optimal torrefaction temperature. In this study, the optimum temperature calculated from correlation equations in Figures 1 and 2 was found to be 240 ºC, in accordance with the work of Agarwal *et al.* [40].

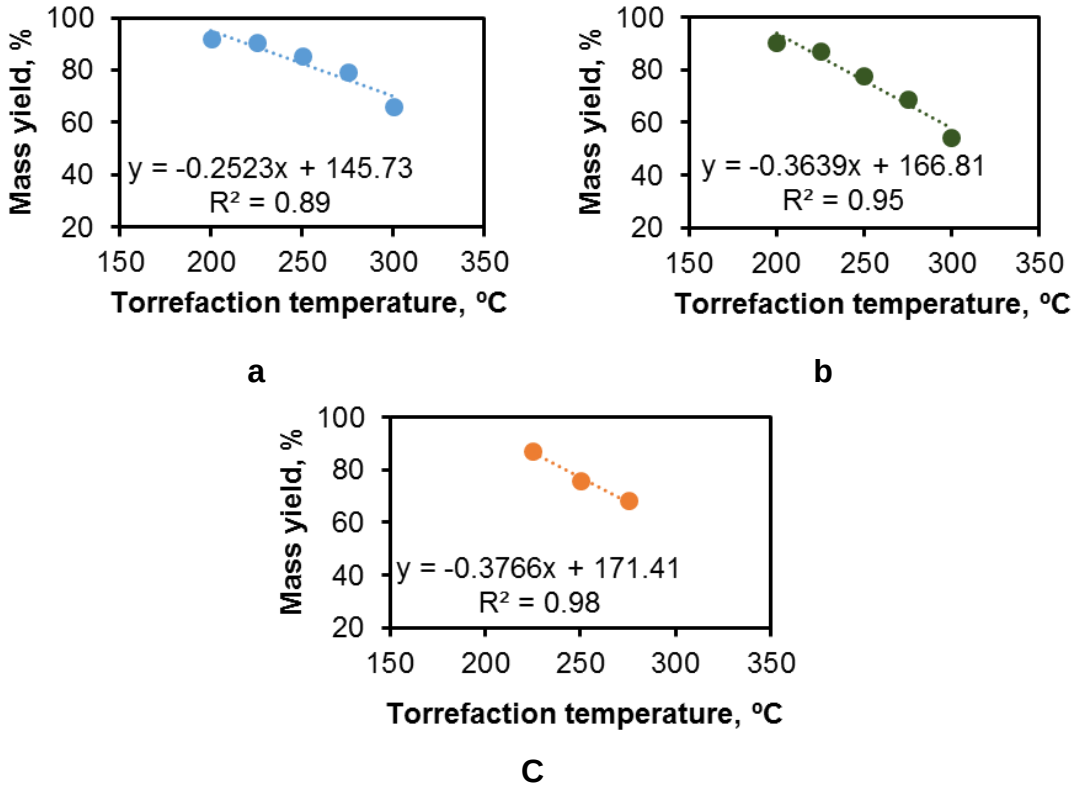

178 Figure 1. Relationship between mass yield and torrefaction temperature of a)
179 pine, b) eucalyptus and c) chestnut.

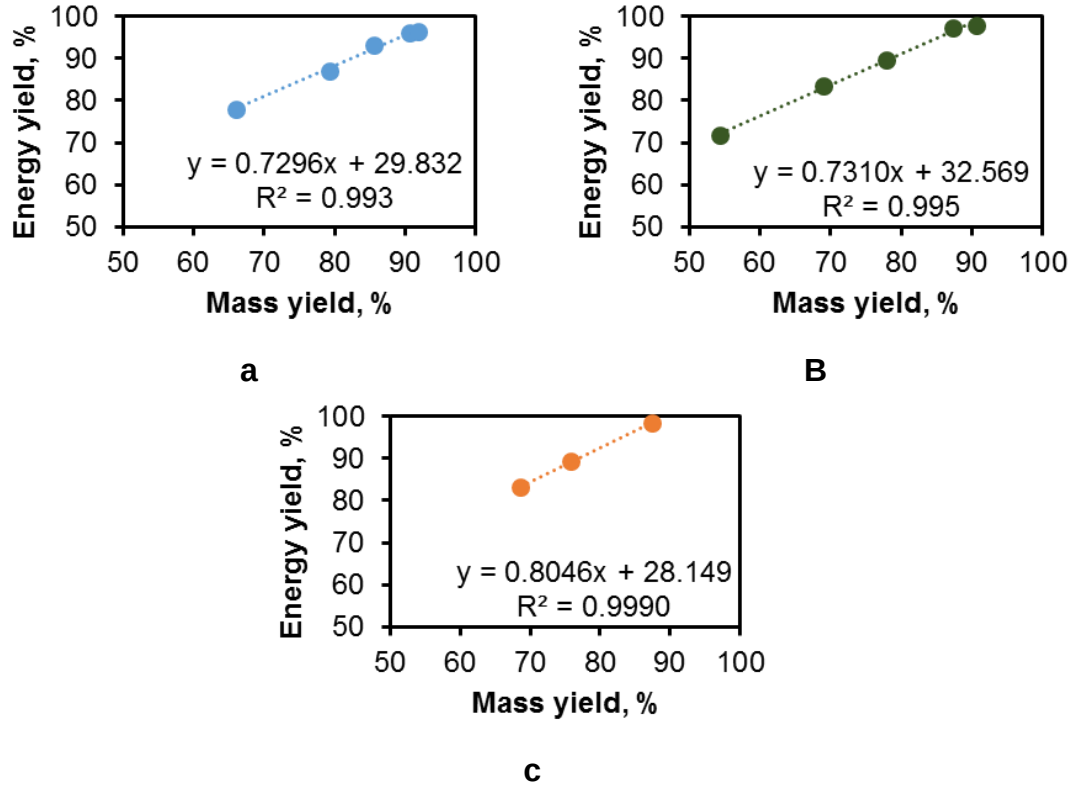

180 Figure 2. Relationship between energy yield and mass yield of a) pine, b)
181 eucalyptus and c) chestnut.

Once the optimum temperature was identified, the torrefaction of the other samples were conducted at 240 ºC. Results show that mass and energy yields are close to the target values, 80 % and 90 % respectively (Table 3).

Table 3. Mass and energy yields and proximate analysis of vine shoot, holm oak and olive tree pruning.

Sample	Vine shoot	Holm oak	Olive tree pruning
Temperature, ºC	240	240	240
HHV, J/g	18840	20254	20759
Mass yield, %	82.9	75.5	77.2
Energy yield, %	94.7	87.2	89.0

The proximate analysis of the six samples (Figure 3) shows that the moisture content decreases as the torrefaction temperature increases and at the optimal temperature, this value is at around 3 %. In Figure 3, there is a general trend of decreasing volatile matter and increasing fixed carbon content as the torrefaction conditions become more severe. Ash content in torrefied biomass is higher than in raw biomass due to the mass loss of organic matter. However, the total amount of ashes decreased after the torrefaction pretreatment as it can be observed in Figure 3, where raw weight basis was used.

The van Krevelen diagram shows the decrease of both atomic ratios O/C and H/C as the torrefaction temperature increases (Figure 4). Carbon is the major source of heat release from combustion while oxygen reduces the calorific value of a fuel. The higher the oxygen contained in a fuel the lower the heating value is. A study of Chen states that the reduction of hydrogen and oxygen contents is due to the removal of moisture and light volatiles which contain more hydrogen and oxygen [42]. A slight increase in O/C ratio for eucalyptus torrefied at 225 ºC is observed in Figure 4, the same behaviour is observed in the work

of Peláez-Samaniego for pine torrefied at 225 ºC [43].

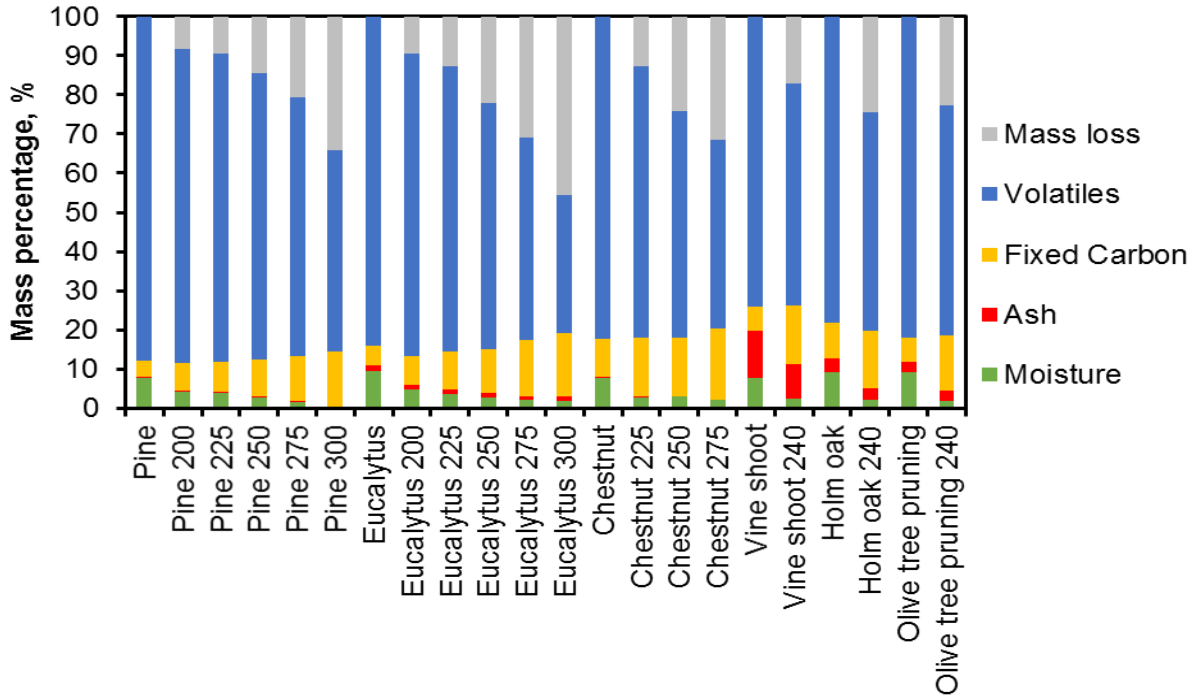

Figure 3. Proximate analysis of the biomass samples for all the torrefaction conditions.

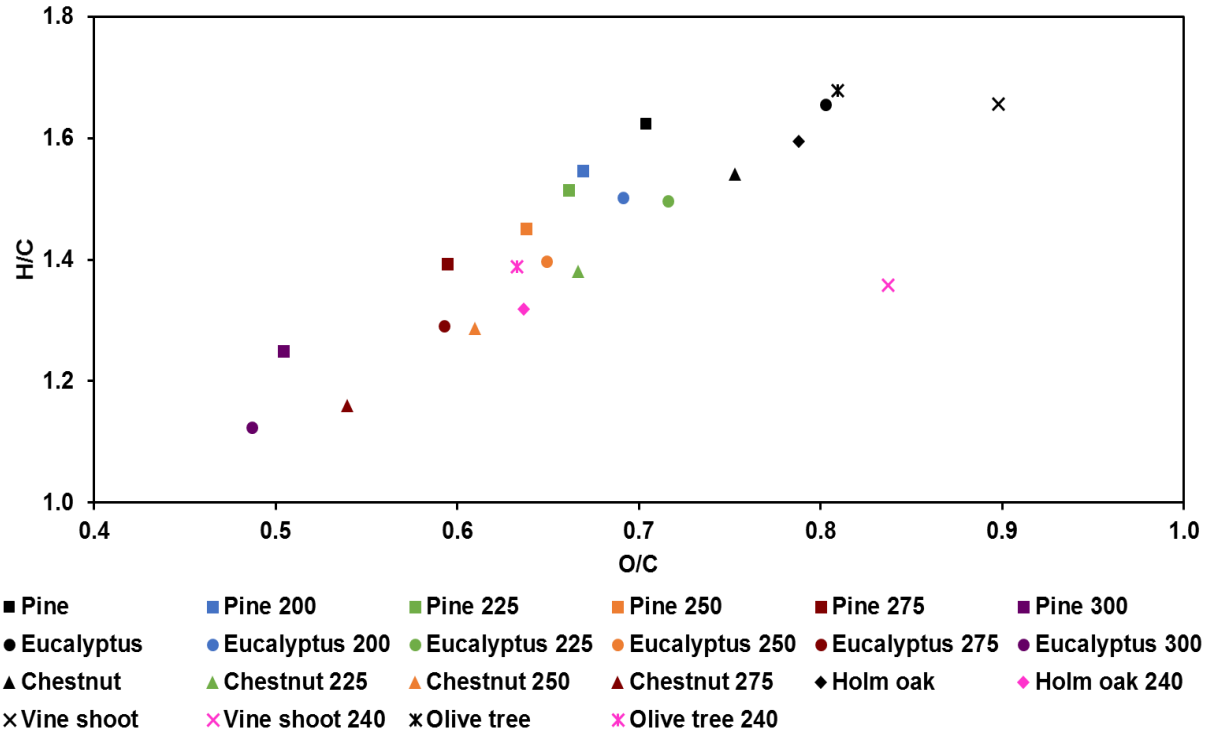

Figure 4. Van Krevelen diagram of biomass samples.

The contact angle measurements showed that there was an overall trend of a positive correlation between the torrefaction temperature and contact angle (Table 4 and Figure 5). The values obtained ranged from 93 ± 3 ° for the raw eucalyptus samples (with no torrefaction treatment) till 118 ± 3 ° obtained with the samples torrefied at 300 °C. In other words, the tendency of the water to wet the surface of the pellet decreased with increasing hydrophobicity. Therefore larger contact angles values were obtained with the eucalyptus wood torrefied at higher temperature indicating its large hydrophobicity what could be explained by several reasons including the breakdown of hemicellulose during torrefaction, a chemical rearrangement, which causes nonpolar unsaturated structures, and tar condensation inside the pores and consequent obstruction of the passage of moist air through the solid, which then avoids the condensation of water vapour [44].

3.2. Gas analysis

The pyrograms of the samples are depicted in Figure 6 and the family compounds were showed on Table 5.Different types of compounds were released at the optimal temperature. Some of them are exclusive for pine wood such as aromatic, resin and terpenoids due to its nature. Sugars and sugar-derived products fraction is not as high as usual since the main decomposition products of cellulose and hemicellulose are carbon dioxide, water and acetic acid, which are not able to be properly identified given the limitations of the equipment described in section 2.4.

233 Table 4. Contact angle measurements for eucalyptus sample.

Sample	Contact angle, º
Raw	93±3
200 ºC	97±5
225 ºC	101±3
250 ºC	106±4
275 ºC	113±2
300 ºC	118±3

234

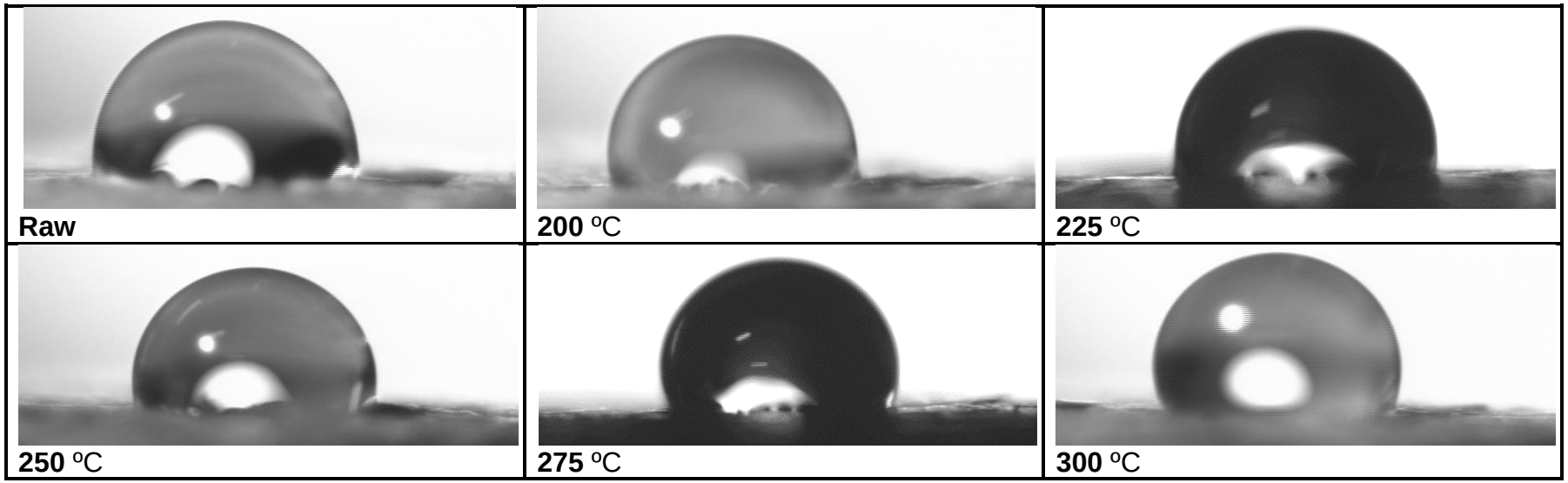

235 Figure 5. Sessile water droplets on the surface of eucalyptus torrefied at different temperatures of torrefaction and raw sample.

236

237 Table 5. Released gases of the samples at 240 ºC from Py-GC-MS as

238 percentage of total chromatographic area.

Type of compound	Pine	Euc.	Chest.	Olive tree	Holm oak	Vine shoot
Aromatic	4.55	0.00	0.00	0.00	0.00	0.00
Lignin (G)	20.31	21.62	32.97	13.33	19.38	21.46
Lignin (H)	0.89	0.00	0.00	2.18	0.00	0.00
Lignin (S)	2.92	44.45	48.26	41.94	43.74	45.93
Lipid	20.14	7.55	5.03	29.91	26.85	20.95
Nitrogenated	0.00	5.92	0.00	2.27	0.00	0.00
Sugars and sugar-derived products	2.53	15.10	11.48	3.85	6.70	4.59
Resin	21.53	0.00	0.00	0.00	0.00	0.00
Sterols	1.00	4.28	2.26	1.28	2.75	4.49
Terpenoids	16.59	0.00	0.00	0.00	0.00	0.00

Euc: Eucalyptus; Chest: Chestnut

239

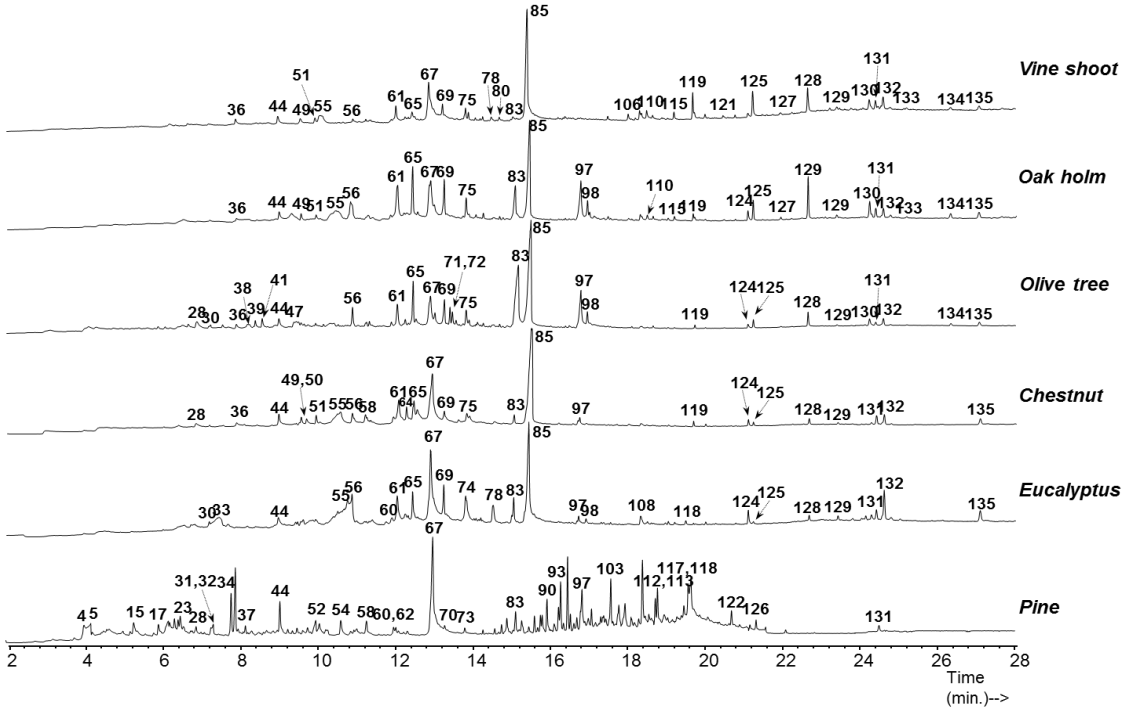

240

241 Figure 6. Pyrograms of the samples. Numbers on the peaks correspond to

242 those in supplementary content.

243

244 Regarding lignin composition, decomposition product from G and S units are

245 the main compounds since all the samples are woody biomass. Decomposition
246 products from H units, which are common in herbaceous samples, were only
247 found in minor amounts in samples of pine wood and olive tree. Pine wood
248 lignin are composed mainly of G units since it is a gymnosperm and in the rest
249 of samples, lignin is composed of both S and G units as these samples are from
250 angiosperms. The main decomposition products from G and S units were the
251 conipheryl aldehyde and sinapaldehyde, respectively (Table S1 in
252 supplementary content). The release of light volatiles such as CO_2 or acetic
253 acid (which were not quantified in the Py-GC/MS experiments) is responsible for
254 the reduction of hydrogen and oxygen contents reported by the ultimate
255 analysis in 3.1. In addition, the products released during torrefaction could have
256 different applications such as the anti-inflammatory effect of conipheryl
257 aldehyde [45] and its ability to promote rapid re-proliferation of the intestinal
258 epithelium [46] or the anti-hyperglycemic and anti-obesity effects of
259 sinapaldehyde [47].

260 **3.3. Kinetics of torrefaction**

261 As the torrefaction is an isothermal process, isothermal kinetics can be
262 obtained. Typically, the conversion-time relationship of a sample is given by
263 equation 1:

$$\frac{d\alpha}{dt} = k(1-\alpha)^n \quad (1)$$

264 where α, which is the conversion of the sample, is defined by:

$$\alpha = \frac{W_i - W}{W_i - W_f} \quad (2)$$

265 where W_i and W_f are the initial (105 ºC) and final (800 ºC) weights of the sample

266 respectively, while W is the weight of the sample at time t.

267 If the order of reaction is unity, the integration of equation 1 gives:

$$ln\left(\frac{1-\alpha_0}{1-\alpha}\right) = k(t-t_0) \quad (3)$$

268 where α_0 is the conversion of the sample at the beginning of torrefaction where

269 $t=t_0$.

270 If the order of reaction is not unity, the integration of equation 1 leads to:

$$(1-\alpha)^{1-n} - (1-\alpha_0)^{1-n} = k(n-1)(t-t_0) \quad (4)$$

271 The order of reaction found is 2.2 and de rate constant, k, is around $4 \cdot 10^{-5}$ s^{-1}

272 (Table 6). This rate constant is close to the value calculated on the basis on the

273 results of Chen and Kuo for hemicellulose at 240 ºC, $6 \cdot 10^{-5}$ s^{-1} [4].

274 Simulations of the conversion of the samples during the torrefaction process

275 were evaluated from Eq. 5 as the order of reaction is not unity:

$$\alpha = 1 - [k(t-t_0)(n-1) + (1-\alpha_0)^{1-n}]^{\frac{1}{1-n}} \quad (5)$$

276 In order to evaluate the reliability of the torrefaction kinetics, simulations and

277 experimental data are compared (Figure 7). The prediction are in good

278 agreement with the experimental data in all the cases.

279 Table 6. Kinetic constant and order of reaction of the torrefaction process.

Sample	n	k [s^{-1}] (x 10^5)	R^2
Pine	2.2	2.17	0.98
Eucalyptus	2.1	3.50	0.98
Chestnut	2.2	4.33	0.97
Vine shoot	2.2	4.50	0.98
Holm oak	2.2	4.83	0.98
Olive tree pruning	2.2	4.17	0.98

280

281

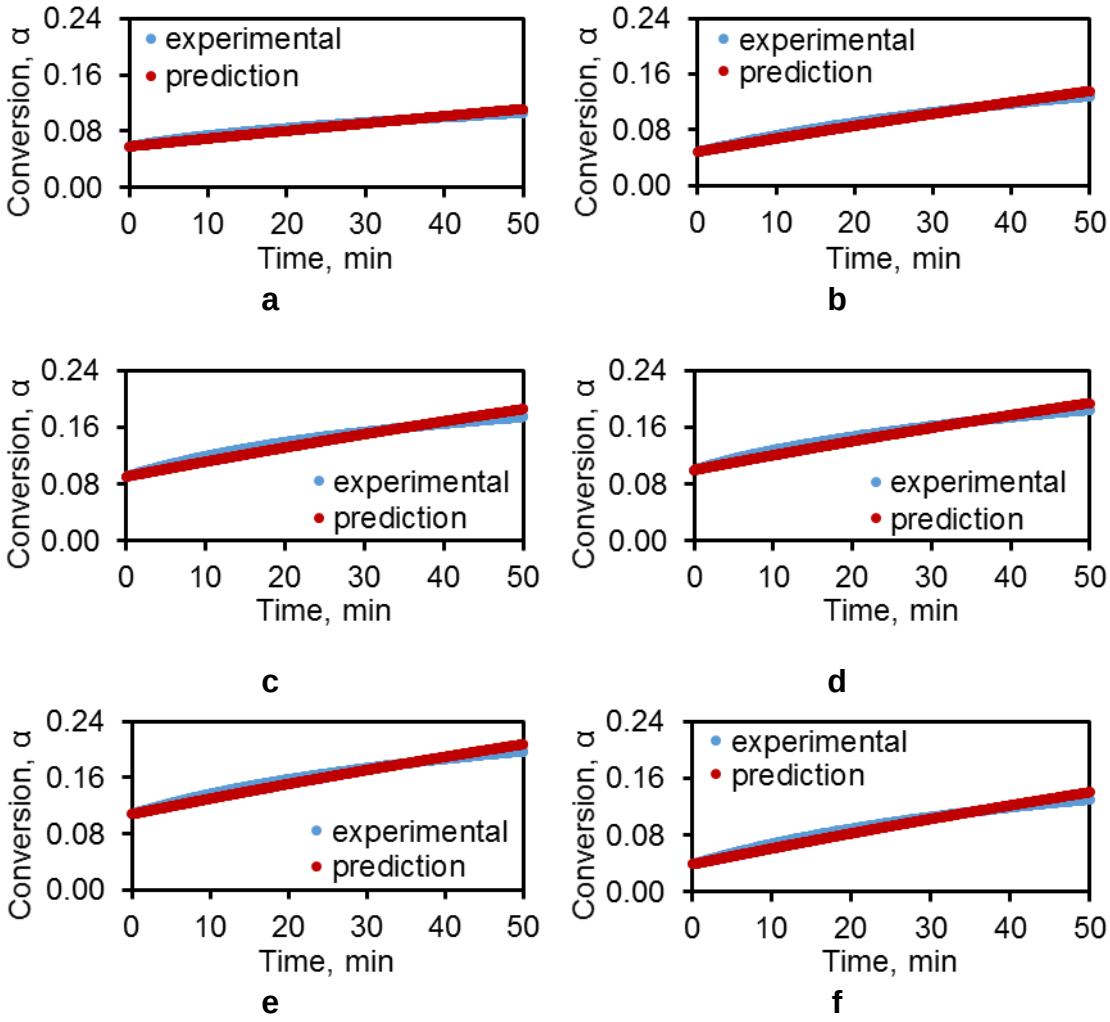

Figure 7. Comparison between predicted and experimental values of a) pine, b) eucalyptus, c) chestnut, d) vine shoot, e) holm oak and f) olive tree pruning.

4. CONCLUSIONS

Biomass samples of some representative forestry and agricultural specimens subjected to a non-oxidative torrefaction process were fully-characterized as energy feedstocks: The optimal torrefaction temperature turned out to be 240 ºC for the target mass and energy yields of 80 % and 90 % respectively. Both the hydrophobicity and the fixed carbon were increased. The decrease of both atomic ratios H/C and O/C was demonstrated through the van Krevelen

292 diagram, which resulted in higher values of HHV. According to Py-GC/MS data,
293 it was demonstrated that there are lignin derivatives compounds in torrefaction
294 gas as well as cellulose and hemicellulose derived compounds.
295 The order of reaction obtained for the six samples was 2.2 and the kinetic
296 constant was around $4 \cdot 10^{-5}$ s^{-1}.
297 These results support the chance of making torrefaction over-costs worthwhile
298 due to the increase of the energetic density of the potential fuel, coming
299 together with the chance of recovering value-added compounds in gas phase.
300

301 **AKNOWLEDGEMENTS**

302 This article is greatly indebted to MINECO for the economic support given to
303 the Normalized vegetable Biomass for Efficient Energetic Trigeneration project
304 (MINECO-13-CTQ2013-45155-R) and Consejería de Economía y Empleo del
305 Principado de Asturias for the economic support given to the TRIBIONOR
306 project (PCTI Asturias 2013–2017, Ref. FC-15-GRUPIN14-095), which makes
307 the continuation of research in this field possible. A. Álvarez acknowledges
308 receipt of a graduate fellowship from the Severo Ochoa Program (Principado de
309 Asturias, Spain).

REFERENCES

[1] Bioenergy 2011. https://www.iea.org/topics/renewables/subtopics/bioenergy/ (accessed August 4, 2016).

[2] Ibrahim RHH, Darvell LI, Jones JM, Williams A. Physicochemical characterisation of torrefied biomass. J Anal Appl Pyrolysis 2013;103:21–30. doi:10.1016/j.jaap.2012.10.004.

[3] Chen W-H. Chapter 10 - Torrefaction. In: Negi S, Binod P, Larroche C, editors. Pretreat. Biomass, Amsterdam: Elsevier; 2015, p. 173–92.

[4] Chen W-H, Kuo P-C. Isothermal torrefaction kinetics of hemicellulose, cellulose, lignin and xylan using thermogravimetric analysis. Energy 2011;36:6451–60. doi:10.1016/j.energy.2011.09.022.

[5] Chen W-H, Kuo P-C. A study on torrefaction of various biomass materials and its impact on lignocellulosic structure simulated by a thermogravimetry. Energy 2010;35:2580–6. doi:10.1016/j.energy.2010.02.054.

[6] Papp EA, Csiha C. Contact angle as function of surface roughness of different wood species. Surf Interfaces 2017;8:54–9. doi:10.1016/j.surfin.2017.04.009.

[7] Morrison ID, Ross S. Colloidal Dispersions: Suspensions, Emulsions, and Foams. Wiley; 2002.

[8] Matos M, Lobo A, Fernández E, Benito JM, Pazos C, Coca J. Recycling of oily ultrafiltration permeates to reformulate O/W emulsions. Colloids Surf Physicochem Eng Asp 2008;331:8–15. doi:10.1016/j.colsurfa.2008.06.004.

[9] Matos M, Lobo A, Benito JM, Coca J, Pazos C. Extending the Useful Life of

Metalworking Fluids in a Copper Wire Drawing Industry by Monitoring Their Functional Properties. Tribol Trans 2012;55:685–92. doi:10.1080/10402004.2012.694580.

[10] Yuan Y, Lee TR. Contact Angle and Wetting Properties. Surf. Sci. Tech., Springer, Berlin, Heidelberg; 2013, p. 3–34. doi:10.1007/978-3-642-34243-1_1.

[11] De Meijer M. A review of interfacial aspects in wood coatings: wetting, surface energy, substrate penetration and adhesion. Proc. Eur. Semin. High Perform. Wood Coat. Exter. Inter. Perform., Paris: 2004, p. 26–7.

[12] Chen W-H, Kuo P-C. Torrefaction and co-torrefaction characterization of hemicellulose, cellulose and lignin as well as torrefaction of some basic constituents in biomass. Energy 2011;36:803–11. doi:10.1016/j.energy.2010.12.036.

[13] Chiou B-S, Valenzuela-Medina D, Bilbao-Sainz C, Klamczynski AK, Avena-Bustillos RJ, Milczarek RR, et al. Torrefaction of pomaces and nut shells. Bioresour Technol 2015;177:58–65. doi:10.1016/j.biortech.2014.11.071.

[14] Matali S, Rahman NA, Idris SS, Yaacob N, Alias AB. Lignocellulosic Biomass Solid Fuel Properties Enhancement via Torrefaction. Procedia Eng 2016;148:671–8. doi:10.1016/j.proeng.2016.06.550.

[15] Phanphanich M, Mani S. Impact of torrefaction on the grindability and fuel characteristics of forest biomass. Bioresour Technol 2011;102:1246–53. doi:10.1016/j.biortech.2010.08.028.

[16] Prins MJ, Ptasinski KJ, Janssen F. Torrefaction of wood - Part 2. Analysis of products. J Anal Appl Pyrolysis 2006;77:35–40.

358 doi:10.1016/j.jaap.2006.01.001.
359 [17] Strandberg M, Olofsson I, Pommer L, Wiklund-Lindström S, Åberg K,
360 Nordin A. Effects of temperature and residence time on continuous
361 torrefaction of spruce wood. Fuel Process Technol 2015;134:387–98.
362 doi:10.1016/j.fuproc.2015.02.021.
363 [18] Gul S, Ramzan N, Hanif MA, Bano S. Kinetic, volatile release modeling and
364 optimization of torrefaction. J Anal Appl Pyrolysis 2017;128:44–53.
365 doi:10.1016/j.jaap.2017.11.001.
366 [19] Shang L, Ahrenfeldt J, Holm JK, Bach LS, Stelte W, Henriksen UB. Kinetic
367 model for torrefaction of wood chips in a pilot-scale continuous reactor. J
368 Anal Appl Pyrolysis 2014;108:109–16. doi:10.1016/j.jaap.2014.05.010.
369 [20] Di Blasi C, Lanzetta M. Intrinsic kinetics of isothermal xylan degradation in
370 inert atmosphere. J Anal Appl Pyrolysis 1997;40:287–303.
371 doi:10.1016/S0165-2370(97)00028-4.
372 [21] Prins MJ, Ptasinski KJ, Janssen FJJG. Torrefaction of wood: Part 1. Weight
373 loss kinetics. J Anal Appl Pyrolysis 2006;77:28–34.
374 doi:10.1016/j.jaap.2006.01.002.
375 [22] Gil MV, García R, Pevida C, Rubiera F. Grindability and combustion
376 behavior of coal and torrefied biomass blends. Bioresour Technol
377 2015;191:205–12. doi:10.1016/j.biortech.2015.04.117.
378 [23] Colin B, Dirion J-L, Arlabosse P, Salvador S. Quantification of the
379 torrefaction effects on the grindability and the hygroscopicity of wood chips.
380 Fuel 2017;197:232–9. doi:10.1016/j.fuel.2017.02.028.
381 [24] Gao N, Li A, Quan C, Du L, Duan Y. TG–FTIR and Py–GC/MS analysis on

pyrolysis and combustion of pine sawdust. J Anal Appl Pyrolysis 2013;100:26–32. doi:10.1016/j.jaap.2012.11.009.

[25] Ghalibaf M, Lehto J, Alén R. Fast pyrolysis of hot-water-extracted and delignified silver birch (Betula pendula) sawdust by Py-GC/MS. J Anal Appl Pyrolysis 2017;127:17–22. doi:10.1016/j.jaap.2017.09.008.

[26] Gu X, Ma X, Li L, Liu C, Cheng K, Li Z. Pyrolysis of poplar wood sawdust by TG-FTIR and Py–GC/MS. J Anal Appl Pyrolysis 2013;102:16–23. doi:10.1016/j.jaap.2013.04.009.

[27] Almeida G, Brito JO, Perré P. Alterations in energy properties of eucalyptus wood and bark subjected to torrefaction: The potential of mass loss as a synthetic indicator. Bioresour Technol 2010;101:9778–84. doi:10.1016/j.biortech.2010.07.026.

[28] Arias B, Pevida C, Fermoso J, Plaza MG, Rubiera F, Pis JJ. Influence of torrefaction on the grindability and reactivity of woody biomass. Fuel Process Technol 2008;89:169–75. doi:10.1016/j.fuproc.2007.09.002.

[29] Arteaga-Pérez LE, Segura C, Bustamante-García V, Gómez Cápiro O, Jiménez R. Torrefaction of wood and bark from Eucalyptus globulus and Eucalyptus nitens: Focus on volatile evolution vs feasible temperatures. Energy 2015;93, Part 2:1731–41. doi:10.1016/j.energy.2015.10.007.

[30] Arteaga-Pérez LE, Segura C, Espinoza D, Radovic LR, Jiménez R. Torrefaction of Pinus radiata and Eucalyptus globulus: A combined experimental and modeling approach to process synthesis. Energy Sustain Dev 2015;29:13–23. doi:10.1016/j.esd.2015.08.004.

[31] Chen W-H, Kuo P-C, Liu S-H, Wu W. Thermal characterization of oil palm

406 fiber and eucalyptus in torrefaction. Energy 2014;71:40–8.
407 doi:10.1016/j.energy.2014.03.117.
408 [32] Nachenius RW, van de Wardt TA, Ronsse F, Prins W. Torrefaction of pine
409 in a bench-scale screw conveyor reactor. Biomass Bioenergy 2015;79:96–
410 104. doi:10.1016/j.biombioe.2015.03.027.
411 [33] Rodrigues A, Loureiro L, Nunes LJR. Torrefaction of woody biomasses
412 from poplar SRC and Portuguese roundwood: Properties of torrefied
413 products. Biomass Bioenergy 2018;108:55–65.
414 doi:10.1016/j.biombioe.2017.11.005.
415 [34] Li M-F, Chen L-X, Li X, Chen C-Z, Lai Y-C, Xiao X, et al. Evaluation of the
416 structure and fuel properties of lignocelluloses through carbon dioxide
417 torrefaction. Energy Convers Manag 2016;119:463–72.
418 doi:10.1016/j.enconman.2016.04.064.
419 [35] Martín-Lara MA, Ronda A, Zamora MC, Calero M. Torrefaction of olive tree
420 pruning: Effect of operating conditions on solid product properties. Fuel
421 2017;202:109–17. doi:10.1016/j.fuel.2017.04.007.
422 [36] ASTM D1102-84(2013). Standard Test Method for Ash in Wood. West
423 Conshohocken, PA: ASTM International; 2013.
424 [37] ASTM E711-87(2004). Standard Test Method for Gross Calorific Value of
425 Refuse-Derived Fuel by the Bomb Calorimeter (Withdrawn 2004). West
426 Conshohocken, PA: ASTM International; 1987.
427 [38] ASTM E871-82(2013). Standard Test Method for Moisture Analysis of
428 Particulate Wood Fuels. West Conshohocken, PA: ASTM International;
429 2013.

[39] ASTM E872-82(2013). Standard Test Method for Volatile Mater in the Analysis of Particulate Wood Fuels. West Conshohocken, PA: ASTM International; 2013.

[40] Agarwal AK, Pandey A, Gupta AK, Aggarwal SK, Kushari A. Novel Combustion Concepts for Sustainable Energy Development. 1st ed. India: Springer; 2014.

[41] Wilén C, Jukola P, Järvinen T, Sipilä K, Verhoeff F, Kiel J, et al. Wood torrefaction: pilot tests and utilisation prospects. Kuopio: 2013.

[42] Chen W-H, Peng J, Bi XT. A state-of-the-art review of biomass torrefaction, densification and applications. Renew Sustain Energy Rev 2015;44:847–66. doi:10.1016/j.rser.2014.12.039.

[43] Pelaez-Samaniego MR, Yadama V, Garcia-Perez M, Lowell E, McDonald AG. Effect of temperature during wood torrefaction on the formation of lignin liquid intermediates. J Anal Appl Pyrolysis 2014;109:222–33. doi:10.1016/j.jaap.2014.06.008.

[44] Basu P. Chapter 4 - Torrefaction. Biomass Gasif. Pyrolysis Torrefaction Second Ed., Boston: Academic Press; 2013, p. 87–145. doi:10.1016/B978-0-12-396488-5.00004-6.

[45] Akram M, Kim K-A, Kim E-S, Shin Y-J, Noh D, Kim E, et al. Selective inhibition of JAK2/STAT1 signaling and iNOS expression mediates the anti-inflammatory effects of coniferyl aldehyde. Chem Biol Interact 2016;256:102–10. doi:10.1016/j.cbi.2016.06.029.

[46] Jeong Y-J, Jung MG, Son Y, Jang J-H, Lee Y-J, Kim S-H, et al. Coniferyl aldehyde attenuates radiation enteropathy by inhibiting cell death and

promoting endothelial cell function. PloS One 2015;10:e0128552. doi:10.1371/journal.pone.0128552.

[47] Camacho S, Michlig S, de Senarclens-Bezençon C, Meylan J, Meystre J, Pezzoli M, et al. Anti-obesity and anti-hyperglycemic effects of cinnamaldehyde via altered ghrelin secretion and functional impact on food intake and gastric emptying. Sci Rep 2015;5:7919. doi:10.1038/srep07919.